Islanded operation of an inverter dominated coupled multi-energy system

Edgar Diego Gomez Anccas*, Johannes Blanz, Detlef Schulz
Helmut-Schmidt-University / University of the Federal Armed Forces Hamburg
Professorship of Electrical Power Systems
*diego.gomez@hsu-hh.de

***Abstract* – The transition from fossil energy to renewables creates challenges concerning grid resilience due to the volatility of power generation based on solar and wind energy and the loss of inertia from synchronous machines. To tackle the temporal and spatial discrepancies between generation and consumption of renewables additional energy storage is necessary. A promising solution is the coupling of different energy sectors, especially gas and electricity, in order to support the sensitive electric grid through gas-to-power technologies such as fuel cells and the possibility to store surplus of electrical energy using power-to-gas technologies such as electrolysers. Even though research on these technologies is steadily advancing the dynamic interactions in strongly coupled systems is not fully understood. This work focuses on islanded microgrids consisting of a hydrogen and electric system coupled through a fuel cell system that is used to set up grid voltage and frequency. The system is simulated in order to test its functionality as grid forming unit during dynamic load changes and volatile power injection via a PV system.**

***Keyword* – Multi-energy-system, inverter-dominated island grid, sector coupling, grid-forming fuel cell operation**

NOMENCLATURE

FC	Fuel cell
H_2	Hydrogen
LV	Low voltage
GtP	Gas-to-Power
MPPT	Maximum-Power-Point-Tracking
PtG	Power-to-Gas
PV	Photovoltaic
REDIBEL	Reversibel-Digital-gekoppelte-Brennstoffzelle-und-Elektrolyse (Engl. Reversible-Digitally-coupled-Fuel Cell-and-Electrolyser)
SM	Synchronous Machine

I. INTRODUCTION

Decarbonization of the existing electrical energy system leads to an increasing share of volatile renewables in the energy mix. To ensure grid stability and reliability of supply under these conditions the whole field of energy storage will have to play a more prominent role [1]. In addition to the temporal volatility of renewable energy sources, their efficiency depends on their geographical location [2, 3]. A promising solution to the temporal and spatial challenges of modern energy grids is the coupling of the energy sectors to multi-energy systems [4]. This is realized using an electrical grid, fed by different energy sources, e.g., electron- and gas-based energy carriers, which are coupled with technologically suitable conversion technologies. The possibility to redistribute energy amongst and share energy storage capabilities across different sectors leads to increased flexibility in all the energy sectors coupled in the here proposed fashion [5]. Political incentives in the context of the *Nationale Wasserstoffstrategie* (Climate Action Programme putting hydrogen centre stage to achieve an energy mix consisting of 100 % renewables) in Germany encourages the use of hydrogen (H_2) as a key energy carrier in future energy systems [6]. Bidirectional energy flow between gas and electric sectors can be achieved using coupling technologies for Power-to-Gas (PtG) and Gas-to-Power (GtP) operations such as electrolysers and fuel cells (FC), respectively. However, due to different dynamic properties of those two technologies and the requirement of power electronics to connect the DC-based coupling technologies to the electric system intelligent control mechanisms are necessary [7].

The research project CoupleIT! aims to create a laboratory and simulation environment in order to investigate dynamic interactions between electric and H_2 systems coupled by a REDIBEL (Reversible-Digitally-coupled-Fuel Cell-and-Electrolyser)-system. The planned microgrid is depicted in FIGURE 1. The research is focused on the behaviour under the rough conditions of islanding operation with volatile PV supply and dynamic load changes. In this work a low voltage AC-microgrid consisting of a FC-system in parallel to a PV system and an AC-load is operated in islanded mode in a simulation environment. In section II of this paper the necessary control methods in order to operate the microgrid in islanded operation are presented. Section III presents the models used in the simulation followed by section IV elaborating on the test cases and simulation results. Finally, the conclusion summarises the results and the outlook offers a glance into the project's future.

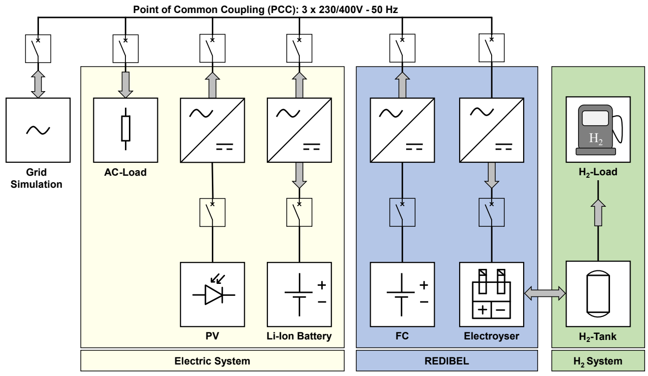

FIGURE 1: MULTI-ENERGY-MICROGRID CONSISTING OF TWO ISLANDED ENERGY SYSTEMS COUPLED BY THE REDIBEL-SYSTEM.

II. METHODS

A. Grid-Feeding Control – PV

Grid-feeding control operates converters by defining values for active and reactive power that is injected to the grid. Additionally, these converters can contribute to the voltage and frequency control in AC-microgrids [8]. PV sources are usually run using grid-feeding control. However, instead of using active and reactive power setpoints a Maximum-Power-Point-Tracking (MPPT)-algorithm is used to yield the maximum output of a PV system. The AC-grid connection is realised via a boost stage and an inverter. The boost stage serves as the PV-side control stage that maximizes the power output of the source. The grid-side control of the inverter balances the DC-link voltage in order to maintain a power equilibrium between PV- and grid-side and preserve the power quality by controlling the supplied grid current [9]. A typical control cascade of a grid-feeding PV-inverter is depicted in FIGURE 2, where v_{dc}^{*} and v_{dc} are the reference and measured DC-link voltages, respectively, i_{dq}^{*} and i_{dq} are the reference and output currents, respectively, and v_{dq}^{*} is the switching node output reference voltage in *dq*-coordinates. Grid-feeding control operates power converters as current sources that require a synchronisation stage to an existing grid. Therefore, grid-feeding converters are reliant on grid-forming, grid-supporting or synchronous machines (SM) to set up both voltage amplitude and frequency [10].

B. Grid-Forming Control – FC

Grids dominated by SMs benefit from the inherent voltage forming and inertial behaviour of the machines. The ability to smoothen frequency deviations utilitsing the kinetic energy stored in the rotor of SMs is to be emulated in some way in future inverter dominated grids lacking said machines. The grid connection of renewable sources needs power electronics with tailored control algorithms in order to emulate the voltage forming and inertial behavior of synchronous machines.

These inverters are called grid-forming inverters. A grid-forming control method that exploits the similarity between a converter and an SM model is called “matching control” [11]. It exploits the important characteristic of the DC bus voltage to reflect power imbalances in a system and uses these as a feedback reference signal.

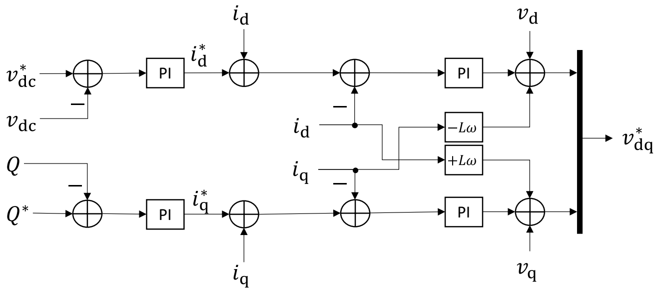

FIGURE 2: GRID-SIDE CONTROL CASCADE OF A GRID-FEEDING PV-INVERTER.

The grid characteristics are set up using a sinusoidal modulation scheme for the AC-voltage reference in *αβ*-coordinates

$$\hat{v}_{\alpha\beta} = \mu \begin{bmatrix} -\sin(\theta) \\ \cos(\theta) \end{bmatrix} \tag{1}$$

with μ and θ as the modulation signal magnitude and angle, respectively. The AC voltage magnitude is controlled using a PI controller

$$\mu = k_{\mathrm{p}}\left(v^{*} - \left\|v_{\mathrm{dq}}\right\|\right) + k_{\mathrm{i}} \int_{0}^{t} \left(v^{*} - \left\|v_{\mathrm{dq}}(\tau)\right\|\right) \mathrm{d}\tau \tag{2}$$

with v_{dq} as the measured AC voltage in *dq*-coordinates. The angular dynamics are derived from the commonalities between converter and SM model in the form of

$$\dot{\theta} = \omega = k_{\theta} v_{\mathrm{dc}} \tag{3}$$

using $k_{\theta} \coloneqq w_0 / v_{\mathrm{dc}}^{*}$ and transforming $\hat{v}_{\alpha\beta}$ to *dq*-coordinates allows the conventional current and voltage cascades being used in control

$$\dot{x}_{\mathrm{vdq}} = \begin{bmatrix} \hat{v}_{\mathrm{d}} - v_{\mathrm{d}} \\ \hat{v}_{\mathrm{q}} - v_{\mathrm{q}} \end{bmatrix} \tag{4}$$

$$i_{sdq}^{*} = \begin{bmatrix} i_{\mathrm{d}} \\ i_{\mathrm{q}} \end{bmatrix} + C\omega \begin{bmatrix} 0 & -1 \\ 1 & 0 \end{bmatrix} \begin{bmatrix} v_{\mathrm{d}} \\ v_{\mathrm{q}} \end{bmatrix} + k_{\mathrm{pv}} \dot{x}_{\mathrm{vdq}} + k_{\mathrm{iv}} x_{\mathrm{vdq}} \tag{5}$$

Where i_{sdq}^{*}, i_{dq}, $\hat{v}_{\mathrm{dq}}$ and v_{dq} denote switching node reference current, output current, ac voltage reference and measurement ac voltage, respectively, in *dq*-coordinates. The proportional and integral gain are denoted by k_{pv} and k_{iv}, respectively. Using i_{dq}^{*} the current loop can be derived as

$$\dot{x}_{\mathrm{idq}} = \begin{bmatrix} i_{\mathrm{sd}}^{*} - i_{\mathrm{sd}} \\ i_{\mathrm{sq}}^{*} - i_{\mathrm{sq}} \end{bmatrix} \tag{6}$$

$$v_{\mathrm{sdq}}^{*} = \begin{bmatrix} v_{\mathrm{d}} \\ v_{\mathrm{q}} \end{bmatrix} + L\omega \begin{bmatrix} 0 & -1 \\ 1 & 0 \end{bmatrix} \begin{bmatrix} i_{sd} \\ i_{sq} \end{bmatrix} + k_{\mathrm{pi}} \dot{x}_{\mathrm{idq}} + k_{\mathrm{ii}} x_{\mathrm{idq}} \tag{7}$$

where v_{sdq}^{*} , $i_{\mathrm{sdq}} = \left[i_{\mathrm{sd}}, i_{sq}\right]^{\top}$, k_{pi} and k_{ii} are reference switching node voltage, switching node current, proportional and integral gains, respectively.

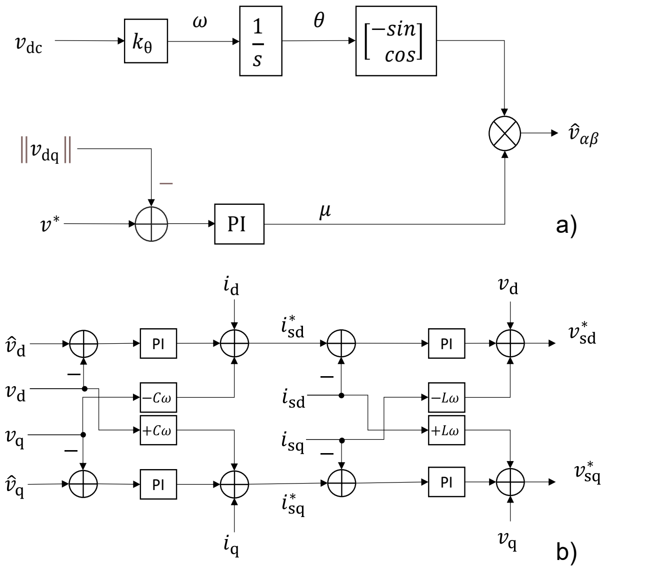

FIGURE 3: BLOCK DIAGRAMS OF THE MATCHING CONTROL A) AND THE CASCADED CONTROL DESIGN B) OF THE INVERTER.

An FC-system can be used as a grid-forming source owing to its reliable and controllable output that is only dependent on the supply of reactants. However, dynamic operation adversely affects an FC's longevity. For this reason, a supporting element is necessary to smooth steep output gradients [12].

C. Grid Simulations

The simulation environment for the coupled energy systems is MATLAB/Simulink® as well as the SimPowerSystems and Thermolib Toolboxes for power systems and thermodynamic simulations, respectively [13].

III. MODELS

The investigated model consists of an FC system run as grid-forming unit using the controller aspects described in II.B to set up a low voltage (LV) 230/400 V, 50 Hz AC-microgrid. The FC system is connected in parallel to a PV system operated in grid-feeding mode according to section II.A. The two sources feed an AC load.

A. FC-Model

The FC-model includes an anode, a cathode, a heat transfer and an energy calculation system. The voltage of a single cell is defined by the following equation:

$$v_{\mathrm{fc}} = E - v_{\mathrm{act}} - v_{\mathrm{ohm}} - v_{\mathrm{conc}} \tag{8}$$

where E is the Nernst voltage, v_{act} the activation losses, v_{ohm} the ohmic losses and v_{conc} the concentration losses [14]. The Nernst voltage is a function of temperature and oxygen and as well as H_2 partial pressures [15]. The activation losses correspond to the energy required to move electrons and break and form chemical bonds and depends on the partial pressure of oxygen and the temperature of the cell [16]. The ohmic losses correspond to the losses that result from the migration of protons through the membrane and movement of electrons through the electrode and are strongly dependent on temperature and membrane humidity [17, 18]. The concentration losses depend, firstly, on the maximum current density that causes precipitous voltage drops and, secondly, on the actual FC current. The fitting parameters are chosen according to [14, 19, 20]. Under the assumption, that all cells in a stack are identical the stack voltage is calculated by scaling up the single cell voltage by the number of cells n according to

$$v_{\mathrm{st}} = n \cdot v_{\mathrm{fc}}. \tag{9}$$

The stack polarization curve and P/I plot are depicted in FIGURE 4. In this model an ideal supply of H_2, air and coolant is assumed. The link between necessary reactant supply for FC operation is calculated according to [21].

$$\dot{n}_{\mathrm{H}_2} = \frac{I \cdot n}{2 \cdot F} \tag{10.1}$$

$$\dot{n}_{O_2} = 2 \cdot \dot{n}_{\mathrm{H}_2} \tag{10.2}$$

Where $\dot{n}$ is the molar flow of H_2/oxygen per second, I the FC current, n the number of cells and F the Faraday constant. The FC system is connected to a DC/DC stage boosting the FC voltage to the desired v_{dc} and a DC/AC stage that is operated as described in section II.B. The model parameters are summarised in TABLE 1.

B. PV – Model

For the simulation of the PV System the SimPowerSystem PV-Array model is used. The array is structured in five parallel strings each containing 10 modules in series. Each module consists of 60 Cells. The U/I characteristics of a module is derived from the 1 Diode equivalent circuit. The circuit dynamics are described by the following equation.

$$I = I_0 \left(e^{\frac{U}{U_T}} - 1 \right) \tag{11}$$

Where I is the module current, I_0 the saturation current, U the module voltage and U_T the thermal voltage [22]. The PV array is connected to the microgrid through a DC/DC and DC/AC stage. The control described in II.A is used to operate the two stages. A constant temperature of 25 °C and a solar power inflow of 250 to 300 W/m^2 is set. The model data for the PV-array is given in TABLE 2.

TABLE 1: FC MODEL PARAMETER.

Air supply pressure	2 bar
H_2 supply pressure	2 bar
Stack temperature	60° C
Nominal power	6 kW
Number of cells	96
Cell area	165 cm^2

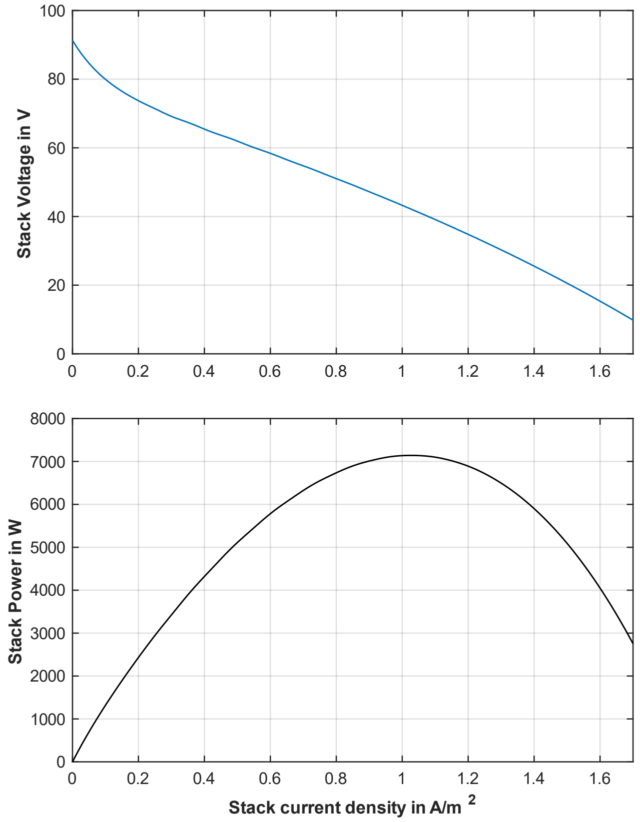

FIGURE 4: POLARIZATION CURVE AND P/I PLOT OF THE STACK

IV. SIMULATIONS

A. Grid-forming Fuel Cell System

The stand-alone grid-forming controlled FC-system feeds a static 3 kW AC-load. The examined fault is a load step ΔP of 1 kW during steady state at $t_{step} = 5$ s. In FIGURE 5 a load increase creates a power imbalance that cannot be compensated by the fuel cell alone (FIGURE 5 a)) and is supplemented by discharging the DC-capacitor and thus decreasing v_{dc} (FIGURE 5 b)). As the grid frequency is derived from v_{dc} a load increase induces an increase in grid frequency, resulting in the desired behaviour of a grid-forming unit (FIGURE 5 c)). In FIGURE 5 d) the power equilibrium between injected active power and load is shown. The matching control of the fuel cell system is able to track the desired load power. However, due to the DC-side control focus on keeping v_{dc} at 700 V and not taking losses into account an offset between P_{Load} and P_{FC} occurs.

TABLE 2: PV MODEL PARAMETER

Parallel strings	5
Modules per string	10
Cells per module	60
Module open circuit voltage	36.3 V
Module short circuit current	7.84 A
Saturation current	2.9273 x 10^{-10} A
Diode ideality factor	0.98119

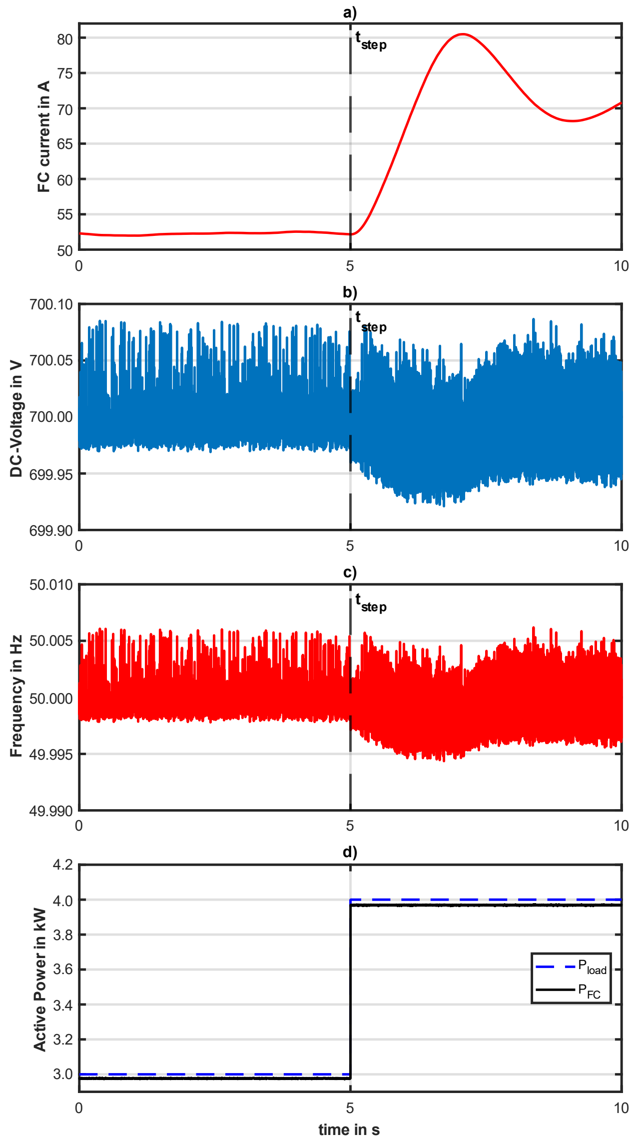

FIGURE 5: RESPONSE OF FC CURRENT a), DC VOLTAGE b), MICROGRID FREQUENCY c), AND ACTIVE POWER d) DURING A LOAD EVENT AT $t_{STEP} = 5$ s.

B. Fuel Cell in parallel to PV during load variation

In the previous section the transient behavior of the grid-forming FC-system during a load step was examined. Now, the long-term behavior of the system during dynamic load changes and variable power injection needs to be investigated. In this section the grid-forming FC System is run in parallel to the PV system described in section III.B. The sources feed an AC-load of 5 kW during 5 hours. The static load pulses by a ΔP of 1 kW every 30 minutes. In FIGURE 6 the system's behaviour can be seen. The load pulsation induces a change in v_{dc} at every pulse event (FIGURE 6 a)). As the PV system is operated in grid-feeding MPPT-mode according to II.A it feeds a defined amount of active power into the grid that depends on temperature and solar irradiance. The temperature is fixed at 25 °C and the irradiance is set to cycle between 250 and 300 W/m^2. In order to meet the experienced load demand, the missing amount is supplied by the FC system (FIGURE 6 b)).

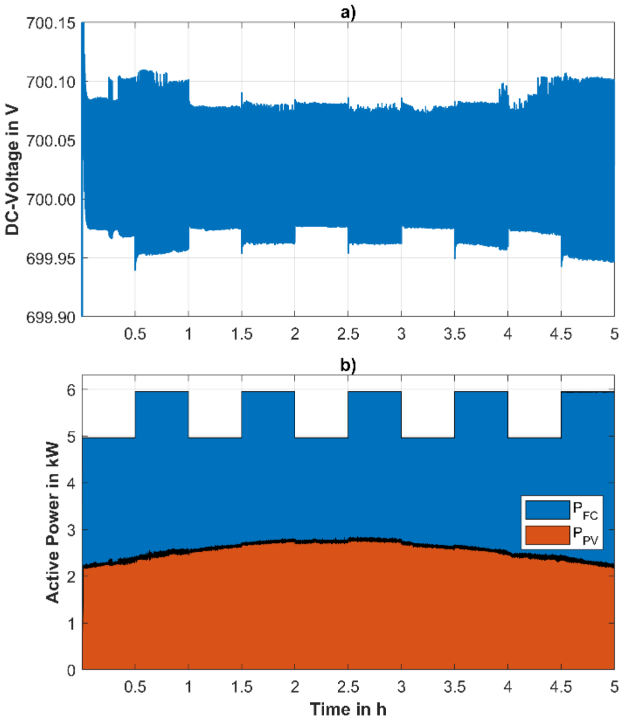

FIGURE 6: DC-LINK VOLTAGE a) AND ACTIVE POWER SUPPLY OF PV (P_{PV}) and FC (P_{FC}) IN b) DURING LOAD PULSES AND VOLATILE POWER INJECTION.

V. Conclusion and Outlook

The aim of the project is to understand the dynamics in a coupled LV AC- and H_2-microgrid in islanded operation. The approach opted for in this work is to employ an FC system as a grid-forming unit as the coupling technology of choice. The matching control technique is selected to operate the grid-forming converter control using a DC reference to derive grid characteristics. The simulation results show that, a stand-alone FC system is able to stabilize the microgrid under transient load events. However, an offset between power injection and consumption is observed due to losses that, as of now, have not been taken into account. Furthermore, a parallel FC and PV system was investigated over an observation period of 5 h. As a result, the grid-forming behavior of the FC system could be validated during volatile energy injection and consumption. Although the results in the simulation environment show that using an FC system with suitable control stabilizes the grid in a power mismatch during short- and long-term events, possible damage to the FC system during load cycling is neglected albeit expected. Additionally, the FC model needs to be extended to include real reactant supply. Thus, future research in the project CoupleIT! will comprise validation of simulation results in a laboratory environment and the inclusion of additional grid-supporting components to reduce the impact of load cycling on the grid forming unit in order to conserve its lifetime.

Acknowledgement

This Paper is funded by dtec.bw – Digitalization and Technology Research Center of the Bundeswehr which we gratefully acknowledge [Project IT-gestützte Sektorenkopplung: Digital gesteuerte Brennstoff-zellen- und Elektrolysetechnologie für stationäre und mobile Anwendungen – CoupleIT!].

VI. References

[1] M. D. Leonard, E. E. Michaelides, and D. N. Michaelides, “Energy storage needs for the substitution of fossil fuel power plants with renewables,” *Renewable Energy*, vol. 145, pp. 951–962, 2020, doi: 10.1016/j.renene.2019.06.066.

[2] J. Drücke *et al.,* “Climatological analysis of solar and wind energy in Germany using the Grosswetterlagen classification,” *Renewable Energy*, vol. 164, pp. 1254–1266, 2021, doi: 10.1016/j.renene.2020.10.102.

[3] F. Masurowski, M. Drechsler, and K. Frank, “A spatially explicit assessment of the wind energy potential in response to an increased distance between wind turbines and settlements in Germany,” *Energy Policy*, vol. 97, pp. 343–350, 2016, doi: 10.1016/j.enpol.2016.07.021.

[4] M. Wietschel, P. Plötz, B. Pfluger, and M. Klobasa, *Sektorkopplung: Definition, Chancen und Herausforderungen.* [Online]. Available (1st September 2022): http://hdl.handle.net/10419/175374

[5] G. Fridgen, R. Keller, M.-F. Körner, and M. Schöpf, “A holistic view on sector coupling,” *Energy Policy*, vol. 147, p. 111913, 2020, doi: 10.1016/j.enpol.2020.111913.

[6] Bundesministerium für Wirtschaft und Energie (BMWi), *Die Nationale Wasserstoffstrategie*. [Online]. Available (1st September 2022): https://www.bmwk.de/Redaktion/DE/Publikationen/Energie/die-nationale-wasserstoffstrategie.pdf?__blob=publicationFile&v=20

[7] Bundesamt für Sicherheit in der Informationstechnik, *Standardisierungsstrategie zur sektorübergreifenden Digitalisierung nach dem Gesetz zur Digitalisierung der Energiewende.* [Online]. Available (1st September 2022): https://www.bmwi.de/Redaktion/DE/Downloads/S-T/standardisierungsstrategie.pdf?__blob=publicationFile&v=4

[8] H. H. Zeineldin, E. F. El-saadany, and M. M. A. Salama, “Distributed Generation Micro-Grid Operation: Control and Protection,” in *2006 Power Systems Conference: Advanced Metering, Protection, Control, Communication, and Distributed Resources*, 2006, pp. 105–111.

[9] J. Rodriguez, Ed., *Advanced and intelligent control in power electronics and drives*: Springer International Publish, 2016.

[10] J. Rocabert, A. Luna, F. Blaabjerg, and P. Rodríguez, “Control of Power Converters in AC Microgrids,” *IEEE Trans. Power Electron.*, vol. 27, no. 11, pp. 4734–4749, 2012, doi: 10.1109/TPEL.2012.2199334.

[11] A. Tayyebi, D. Gross, A. Anta, F. Kupzog, and F. Dorfler, “Frequency Stability of Synchronous Machines and Grid-Forming Power Converters,” *IEEE J. Emerg. Sel. Topics Power Electron.*, vol. 8, no. 2, pp. 1004–1018, 2020, doi: 10.1109/JESTPE.2020.2966524.

[12] G. Wang, F. Huang, Y. Yu, S. Wen, and Z. Tu, “Degradation behavior of a proton exchange membrane fuel cell stack under dynamic cycles between idling and rated condition,” *International Journal of Hydrogen*

Energy, vol. 43, no. 9, pp. 4471–4481, 2018, doi: 10.1016/j.ijhydene.2018.01.020.
[13] EUtech Scientific Engineering GmbH, *Thermolib.* [Online]. Available (1st September 2022): https://www.thermolib.de/
[14] M. J. Grimble, M. A. Johnson, J. T. Pukrushpan, A. G. Stefanopoulou, and H. Peng, *Control of Fuel Cell Power Systems*. London: Springer London, 2004.
[15] J. C. Amphlett, R. M. Baumert, R. F. Mann, B. A. Peppley, P. R. Roberge, and T. J. Harris, “Performance Modeling of the Ballard Mark IV Solid Polymer Electrolyte Fuel Cell: II . Empirical Model Development,” *J. Electrochem. Soc.*, vol. 142, no. 1, pp. 9–15, 1995, doi: 10.1149/1.2043959.
[16] H. Behret, “Karl Kordesch und Günter Simader: Fuel Cells and Their Applications, VCH, Weinheim, 1996. ISBN 3-527-28579-2, DM 248,-,” *Berichte der Bunsengesellschaft für physikalische Chemie*, vol. 100, no. 11, p. 1922, 1996, doi: 10.1002/bbpc.19961001128.
[17] F. Laurencelle *et al.,* “Characterization of a Ballard MK5-E Proton Exchange Membrane Fuel Cell Stack,” *Fuel Cells*, vol. 1, no. 1, pp. 66–71, 2001, doi: 10.1002/1615-6854(200105)1:1<66::AID-FUCE66>3.0.CO;2-3.
[18] J. C. Amphlett, R. M. Baumert, R. F. Mann, B. A. Peppley, P. R. Roberge, and A. Rodrigues, “Parametric modelling of the performance of a 5-kW proton-exchange membrane fuel cell stack,” *Journal of Power Sources*, vol. 49, 1-3, pp. 349–356, 1994, doi: 10.1016/0378-7753(93)01835-6.
[19] T. E. Springer, T. A. Zawodzinski, and S. Gottesfeld, “Polymer Electrolyte Fuel Cell Model,” *J. Electrochem. Soc.*, vol. 138, no. 8, pp. 2334–2342, 1991, doi: 10.1149/1.2085971.
[20] Woong-chul Yang, Bradford Bates, Nicholas Fletcher, and Ric Pow, “Control Challenges and Methodologies in Fuel Cell Vehicle Development,” SAE Technical Paper 98C054, Oct. 1998. [Online]. Available (1st September 2022): https://www.sae.org/publications/technical-papers/content/98c054/
[21] J. Larminie and A. Dicks, *Fuel Cell Systems Explained*. West Sussex, England: John Wiley & Sons, Ltd, 2003.
[22] V. Quaschning, *Regenerative Energiesysteme: Technologie - Berechnung - Klimaschutz,* 11th ed. München: Hanser, 2021. [Online]. Available (1st September 2022): https://www.hanser-elibrary.com/doi/book/10.3139/9783446472068